JOURNAL OF SOLID STATE CHEMISTRY 111, 128–133 (1994)

Synthesis, Structure, and Reactivity of Novel Lanthanum Tungstates

Melitta Gärtner, Dirk Abeln, Allan Pring,[1] Michael Wilde, and Armin Reller[2]

Institute for Inorganic and Applied Chemistry, University of Hamburg, Martin-Luther-King-Platz 6, 20146 Hamburg, Germany

Received November 15, 1993; in revised form February 7, 1994; accepted February 9, 1994
IN HONOR OF C. N. R. RAO ON HIS 60TH BIRTHDAY

Two new compounds, $La_2W_3O_{12}$ and $LaFeW_3O_{12}$, were prepared from La_2O_3 and WO_3 or from Fe_2O_3, La_2O_3, and WO_3. $La_2W_3O_{12}$ has a structure which can be considered as a distorted superstructure of the scheelite structure $CaWO_4$ in which 1/3 of the Ca sites are vacant. It is monoclinic, with space group $C2/c$ and $a = 7.873(2)$ Å, $b = 11.841(2)$ Å, $c = 11.654(2)$ Å, and $\beta = 109.25(3)°$. $LaFeW_3O_{12}$ is triclinic with $a = 7.569(3)$ Å, $b = 7.537(2)$ Å, $c = 32.41(2)$ Å, $\alpha = 90.13(4)°$, $\beta = 94.75(3)°$, and $\gamma = 98.90(3)°$, and the structure consists of two distinct layers, one of which is a La tungstate which consists of a sheet of La in eight coordination and a sheet of WO_4 tetrahedra and another which consists of a sheet of edge-sharing FeO_6 octahedra sandwiched between two sheets of edge-connected WO_6 octahedra. The reactivity of these compounds with H_2 was investigated by TGA. $La_2W_3O_{12}$ is reduced at 1100°C to yield a mixture of La_2O_3 and W metal. The products of the reduction of $LaFeW_3O_{12}$ were found to depend on the composition of the atmosphere. In N_2 with 5% H_2 the compound yields a complex mixture of $La_x(WO_3)_y$ compounds with W and a W–Fe alloy, while in 100% H_2, La_2O_3, W, and the alloys Fe_6W_7 or Fe_2W are formed.

1. INTRODUCTION

Homologous series, in which blocks of perovskite-like oxide structure of various sizes are intergrown with layers of another structure type, are well known. Notable among these series are the so-called Aurivillius and Ruddlesdon–Popper phases (1–4). Recent studies on lanthanum titanates and niobates have revealed another type of perovskite intergrowth structurally based on slabs of perovskite structure of various widths separated by lanthanum–oxygen layers (5–8). In contrast to the Aurivillius and Ruddlesden–Popper phases, which are based on {001} perovskite layers, the new phases are composed of {110} perovskitic layers. Closely related to these phases are the intergrowths based on slabs of corner-connected WO_3, which differ from the perovskites in that they lack large cations in the 8 or 12 coordinated site (5). We attempted to prepare a new type of intergrowth structure consisting of blocks of $LaFeO_3$ perovskite and WO_3. The compounds we prepared, $La_2W_3O_{12}$ and $LaFeW_3O_{12}$, do not have perovskite-related structures.

$La_2W_3O_{12}$ has a structure based on a cation-deficient superstructure of $CaWO_4$. $LaFeW_3O_{12}$ instead adopts a new layer structure which consists of an intergrowth of iron tungstate and lathanum tungstate layers. In this paper we report general structural data and the results of experiments on the thermochemical reactivity of both compounds in H_2.

2. PREPARATION

Both compounds were prepared by heating stoichiometric mixtures of oxides in Pt crucibles in air in a conventional muffle furnace. $La_2W_3O_{12}$ was prepared from La_2O_3 and WO_3 by heating at 1100°C for 5 hr, while $LaFeW_3O_{12}$ was prepared by heating a mixture of La_2O_3, Fe_2O_3, and WO_3 at 1100°C for 12 hr. Since WO_3 melts at approximately 900°C it serves as a flux for crystal growth in both preparations. Slow cooling of the mixtures to room temperature also served to promote crystal growth. $La_2W_3O_{12}$ is colorless while $LaFeW_3O_{12}$ is honey yellow in color and has a submetallic luster and a perfect cleavage on (001).

3. STRUCTURE ANALYSIS

The X-ray diffraction powder patterns were recorded on a Philips automated powder diffractometer using Cu$K\alpha$ radiation. The powder pattern for $La_2W_3O_{12}$ was a good match with the previously published data for this compound and the group of isostructural rare earth tungstates such as $Eu_2W_3O_{12}$ (9). The powder pattern for $LaFeW_3O_{12}$ was indexed with the aid of data from the single-crystal X-ray diffraction and electron diffraction studies. The unit cell parameters were refined by standard least-squares methods. These data are presented in Table 1.

[1] On leave from Department of Mineralogy, South Australian Museum, North Terrace, Adelaide, South Australia 5000, Australia.

[2] To whom correspondence should be addressed.

0022-4596/94 $6.00

TABLE 1
Powder X-Ray Diffraction Data for $LaFeW_3O_{12}$

I/I_0	d_{obs} (Å)	d_{calc} (Å)	hkl
4	16.048	16.143	002
1	8.061	8.073	004
1	5.680	5.695	-111
7	5.376	5.382	006
100	4.038	4.038	008
2	3.821	3.823	1-61*
8	3.639	3.940	0-22
3	3.505	3.504	1-17
3	3.387	3.386	-118*
10	3.230	3.226	1-24, -215*
2	3.173	3.173	2-14*
7	3.065	3.055	122, -216
2	2.936	2.934	1-26
3	2.857	2.854	214, -127
2	2.740	2.739	-224, 215
17	2.693	2.696	-209, -2-17
1	2.587	2.587	-226
3	2.455	2.455	0-32, -2-21, -313
19	2.309	2.308	129
1	2.182	2.183	3-15, 2-29
1	2.143	2.141	-3-16
2	2.102	2.101	135
2	2.037	2.036	228
5	2.021	2.024	1-39
2	1.966	1.966	3-19
1	1.938	1.937	-1-39
1	1.904	1.901	3-31
2	1.869	1.869	-402
1	1.800	1.799	-337, 3-35
3	1.760	1.763	2-42
1	1.685	1.681	048
3	1.617	1.613	2-48
1	1.563	1.560	335
2	1.509	1.509	337
3	1.485	1.486	051
25	1.471	1.471	053
2	1.431	1.432	-157

Note. Cell parameters refined from the data above: a = 7.569(3) Å, b = 7.537(2) Å, c = 32.41(2) Å, α = 90.13(4)°, β = 94.75(3)°, γ = 98.90(3)°. Volume = 1820(1) Å^3.

$La_2W_3O_{12}$ is isomorphous with a number of rare earth tungstates; however, only the structure of the Eu compound has been studied in detail (10) and so a refinement of the La compounds was undertaken. Intensity data for $La_2W_3O_{12}$ were collected on a rebuilt Hilger & Watts (11, 12) four circle diffractometer with Mo$K\alpha$. Reflections (1474) were collected, from which a data set of 697 independent significant reflections were used for the refinement after data reduction. Absorption was corrected by employing a semiempirical ψ-scan method. The structure was solved by Patterson methods using SHELXS-90 (13) and refined using SHELXL-93 (14). The crystal data for this compound are summarized in Table 2. Atomic coordinates, thermal parameters, and selected bond lengths as well as angle data are presented in Tables 3 and 4.

TABLE 2
Crystal Data and Results of Crystal-Structure Refinement for $La_2W_3O_{12}$

Crystal size	0.1 × 0.1 × 0.2 mm
Unit cell dimensions	
a (Å)	7.873(2)
b (Å)	11.841(2)
c (Å)	11.654(2)
β	109.25(3)°
V (Å^3)	1025.7(4)
Z	4
Space group	$C2/c$ (No. 15)
D_{calc} (g cm^{-3})	6.614
μ (mm^{-1})	41.724
$F(000)$	1728
Radiation Mo$K\alpha$	0.71073 Å
Collection limit	
θ(Mo$K\alpha$)	3.24° to 22.55°
Index range	$0 \le h \le 8$, $-12 \le k \le 12$, $-12 \le l \le 11$
Unique reflections	697
R ($I > 2\sigma(I)$)	0.0499
wR^2	0.1210
Residual peak	3.537 $e \cdot$ Å^{-3}
Hole	-2.514 $e \cdot$ Å^{-3}

$La_2W_3O_{12}$ has a distorted scheelite structure in which the W atoms are in tetrahedral coordination with O, while La has eight oxygen nearest neighbors. The WO_4 tetrahedra are arranged around the La atoms in a tetrahedral arrangement.

Only a summarizing account of the crystal structure of $LaFeW_3O_{12}$ will be given here as full details of the refinement will be published elsewhere (15). $LaFeW_3O_{12}$ crystallizes in a triclinic unit cell with a = 7.569(3) Å, b = 7.537(2) Å, c = 32.41(2) Å, α = 90.13(4)°, β = 94.75(3)°, γ = 98.90(3)°, and space group $P1$ (No. 1) with Z = 8.

TABLE 3
Atomic Coordinates and Thermal Parameters for $La_2W_3O_{12}$

	x	y	z	U(eq)
La	3200(2)	3737(1)	4041(1)	21(1)
W(1)	1531(2)	3538(1)	460(1)	21(1)
W(2)	5000	6185(1)	2500	23(1)
O(1)	6205(23)	2891(19)	4246(13)	26(5)
O(2)	688(27)	3009(18)	4639(15)	33(5)
O(3)	2175(27)	4240(17)	1879(16)	28(5)
O(4)	1851(26)	2037(18)	2787(15)	33(5)
O(5)	1392(26)	5409(19)	4393(15)	31(5)
O(6)	5132(23)	5404(16)	3856(15)	24(4)

Note. Atomic coordinates (×10^4) and equivalent displacement parameters (Å^2 × 10^3). U(eq) is defined as one-third the trace of the orthogonalized U_{ij} tensor.

TABLE 4
Selected Bond Lengths and Angles for $La_2W_3O_{12}$

Bonds	Lengths (Å)
La–O(3)	2.45(2)
–O(2)	2.46(2)
–O(4)	2.51(2)
–O(2)	2.55(2)
–O(6)	2.55(2)
–O(5)	2.55(2)
–O(6)	2.58(2)
W(1)–O(5)	1.74(2)
–O(3)	1.77(2)
–O(2)	1.82(2)
–O(1)	1.87(2)
–O(1)	2.17(2)
W(2)–O(4)	1.71(2)
–O(4)	1.71(2)
–O(6)	1.80(2)
–O(6)	1.80(2)
Bonds	**Angles**
O(5)–W(1)–O(3)	105.2(9)°
O(5)–W(1)–O(2)	111.6(9)°
O(3)–W(1)–O(2)	101.2(9)°
O(5)–W(1)–O(1)	104.9(9)°
O(4)–W(2)–O(6)	109.4(8)°
O(4)–W(2)–O(6)	105.8(8)°
O(4)–W(2)–O(6)	109.4(8)°
O(4)–W(1)–O(6)	105.8(9)°

The structure consists of an intergrowth of two layers: an $La_2W_2O_9$ layer composed of sheets of edge-sharing LaO_8 polyhedra (highly distorted monocapped trigonal prisms), which is linked via corner sharing to a sheet of WO_4 tetrahedra. The second layer, of composition $Fe_2W_4O_{15}$, consists of sheets of edge-sharing FeO_6 octahedra sandwiched between two sheets of edge-connected WO_6 octahedra. The layers which are stacked parallel to (001) in the sequence $La_2W_2O_9$, $Fe_2W_4O_{15}$, $La_2W_2O_9$, $Fe_2W_4O_{15}$ along the 32-Å c repeat (see Fig. 1). Thus the compound contains W in both tetrahedral and octahedral coordination. High-resolution electron micrographs taken along the c axis give evidence for perfect ordering (Fig. 2). As revealed by selected area electron diffraction patterns, partial stacking faults of the $La_2W_2O_9$ and $Fe_2W_4O_{15}$ layers parallel to (001) must be suggested.

4. THERMOCHEMICAL REACTIVITY

The thermochemical reactivities of these tungstates were investigated in various atmospheres using combined TG/DTA thermal analyzers (Netzsch STA 409 as well as Mettler TA2000). The products of the reactions were identified by powder X-ray diffraction, electron diffraction, and energy-dispersive X-ray analysis.

In the case of $La_2W_3O_{12}$ the samples were heated in a stream of 100% H_2 at a heating rate of 10 K per minute from room temperature to 1400 K. The compound undergoes reduction in a two-step process. In a first step a weight loss of 6.2% is measured as intermediates $La_2W_{1.25}O_{6.75}$ (JCDPS 32-503) and W metal are obtained. The reduction of $La_2W_{1.25}O_{6.75}$ leads to the formation of La_2O_3 and again W metal (weight loss, 2.6%). The measured weight loss of the complete reduction under the described conditions is 9.8%.

The reactivity of $LaFeW_3O_{12}$ was studied in more detail.

In a first set of experiments thermogravimetric runs were performed in 100% H_2 (Fig. 3a) at heating rates of 10 $K \cdot min^{-1}$ were used and the reduction was followed up to 1400 K. The TG curve shows that the reduction starts at 780 K. Two shoulders at 1036 and 1127 K indicate the formation of metastable intermediates. The isolation and subsequent characterization of the first intermediate did not yield unambiguous information. As the product of the second reduction step, a mixture of La_2WO_6 and an W–Fe alloy was identified. The corresponding weight loss of

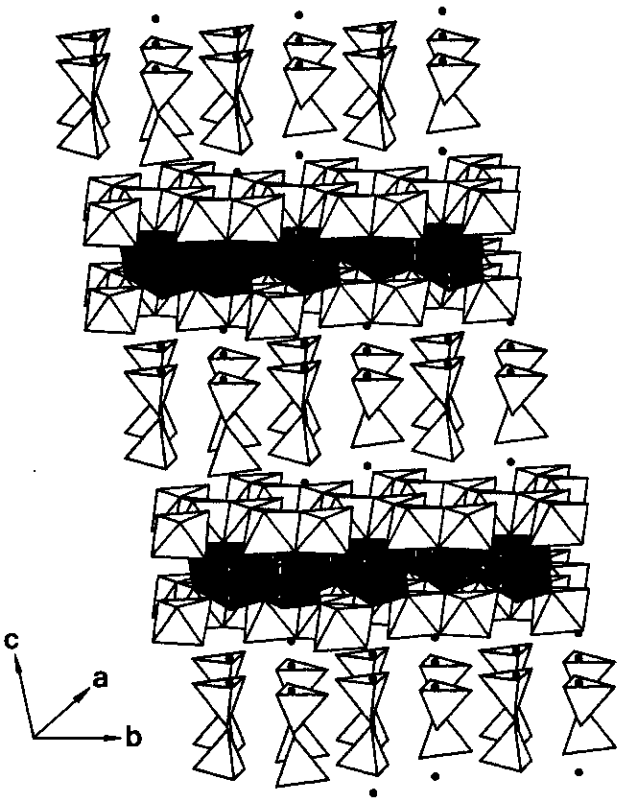

FIG. 1. Schematic diagram of the structure of $LaFeW_3O_{12}$ showing the stacking of $La_2W_2O_9$ and $Fe_2W_4O_{15}$ layers (full circles, La atoms).

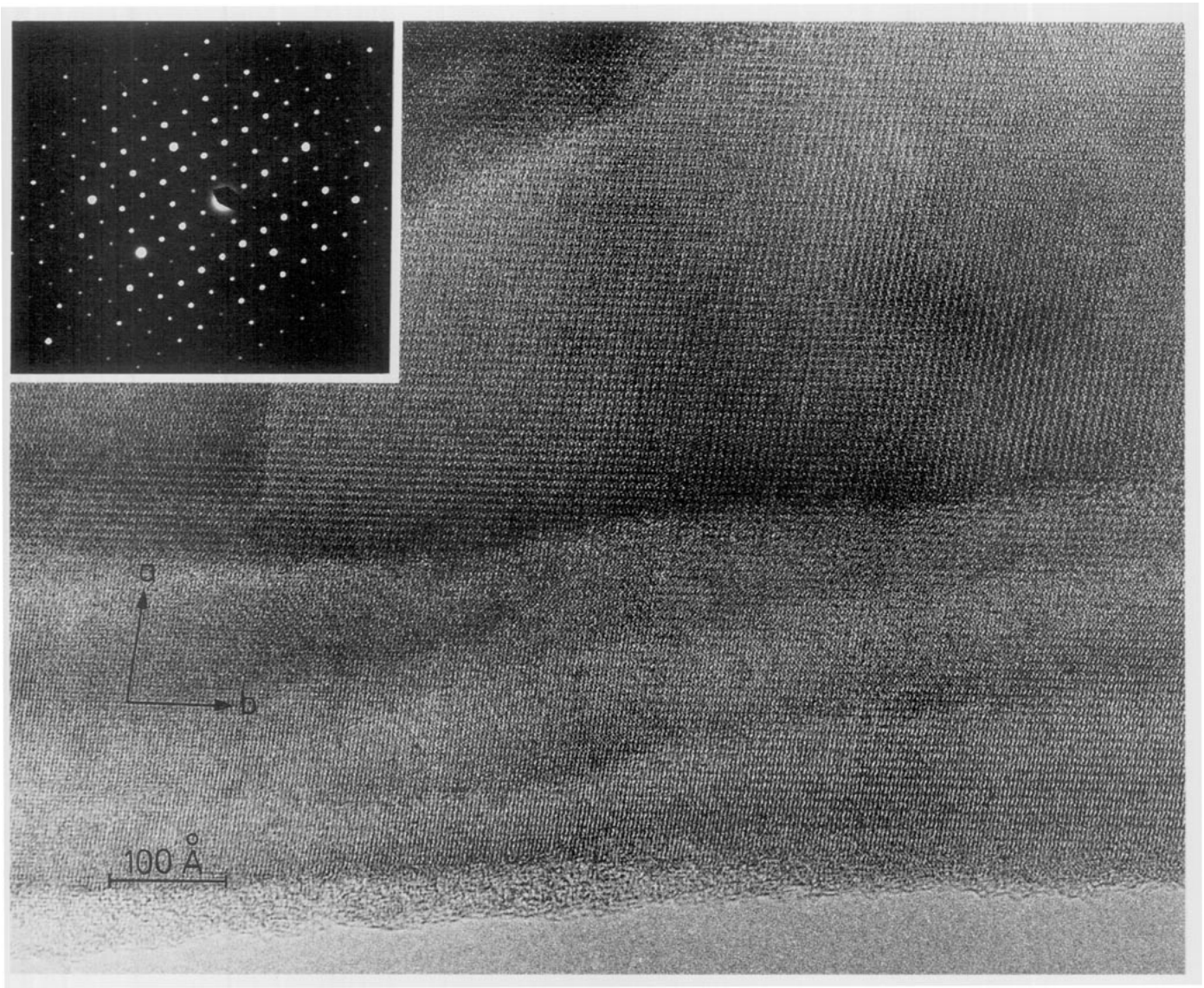

FIG. 2. High-resolution electron micrograph and corresponding selected-area electron diffraction pattern of $LaFeW_3O_{12}$ (projection along (001)).

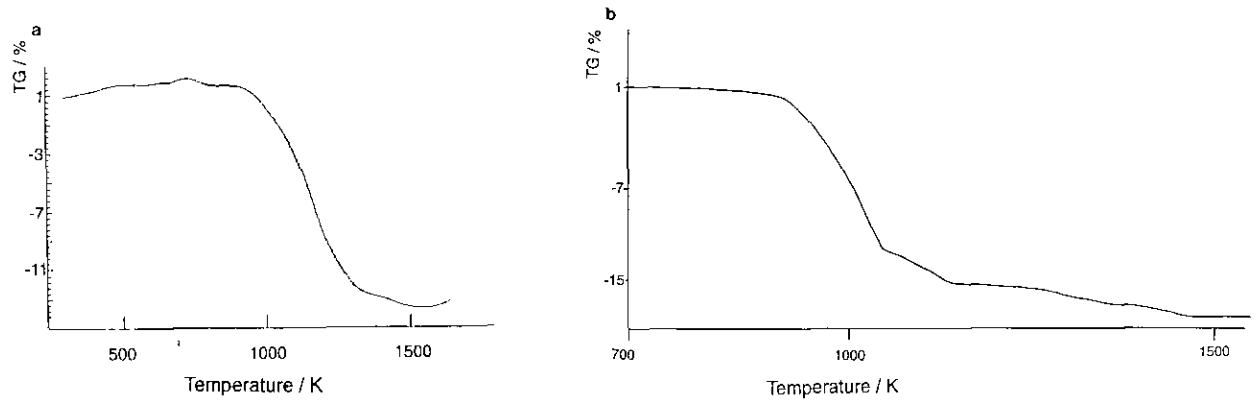

FIG. 3. TG curve for the reduction of microcrystalline $LaFeW_3O_{12}$ in 100% H_2 (a) and of single-crystalline $LaFeW_3O_{12}$ in 5% H_2/95% N_2 (b), both samples heated to 1500 K (heating rate, 10 K · min^{-1}).

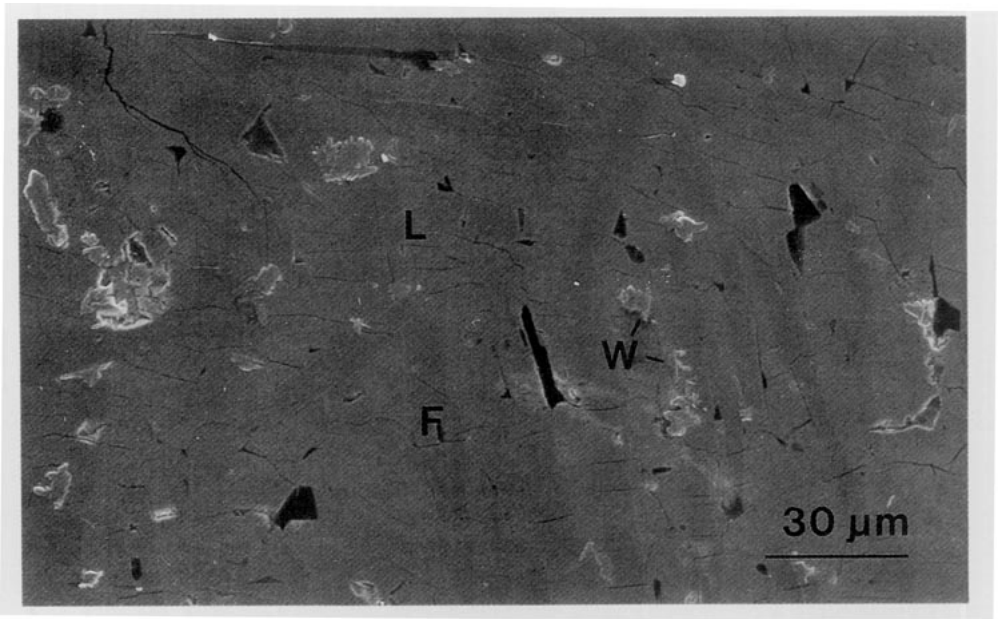

FIG. 4. Scanning electron micrograph showing the products of partial reduction of $LaFeW_3O_{12}$ at 1350°C. The phases are $La_2W_3O_{12}$ (L), $FeWO_4$ (F), and W (W).

14% corresponds to the evolution of approximately eight oxygens per formula unit (theoretical weight loss, 13.65%). After the third reduction step (1400 K), i.e., the evolution of another O, La_2O_3, W metal, and a W–Fe alloy (Fe_6W_7 and/or Fe_2W) are obtained as final products. The measured overall weight loss is 16.9%.

The reduction of $LaFeW_3O_{12}$ was also investigated in a stream of 5% H_2 in N_2. The reaction was followed until 1500 K and the TG trace showed a total weight loss of 15.2%, which corresponds to the loss of just under 9 of the 12 O atoms in the formula unit. Under these conditions $LaFeW_3O_{12}$ reacts to form a complex mixture of $La_x(WO_3)_y$ compounds which were not unambiguously identifiable. In addition to the La tungstates, W metal and a W–Fe alloy, probably Fe_6W_7 or Fe_2W, were also formed.

In order to probe the structural nature of the reduction reaction, experiments were performed using single-crystal fragments of $LaFeW_3O_{12}$. A sample was heated in 5% H_2 to 1200°C until loss of 10 O (weight loss of 16.2%). The TGA curve for this reaction is shown in Fig. 3b. It shows two minor shoulders at 1020 K, associated with a weight loss of 1.7%, and at 1200 K, corresponding to a 2.1% weight loss. The products of the reaction are $La_2W_{1.25}O_{6.75}$, (JCDPS 32-503), W metal, and Fe_6W_7 or Fe_2W.

In an additional experiment a single crystal was reduced in a stream of 5% H_2 in N_2 until a weight loss of 6.5% was observed (which corresponds to the loss of four oxygens per formula unit) and then cooled to room temperature. It was found by scanning electron microscopy and energy-dispersive analysis of X rays that the single-crystal fragment had decomposed to form a polycrystalline mixture of $La_2W_3O_{12}$, $FeWO_4$, and W (Fig. 4).

The quantitative results of the thermogravimetric measurements are summarized in Table 5. The results of the described experiments suggest that the reduction of $LaFeW_3O_{12}$ is a complex multistep process. They clearly confirm that the W in octahedral coordination is more easily reduced than the WO_4 tetrahedra. It is also evident that the breakdown of the $Fe_2W_4O_{15}$ layer proceeds via the reduction of Fe(III) to Fe(II) to form $FeWO_4$ and the

TABLE 5
Quantitative Results for the Thermogravimetric Measurements

Temperature interval[a]	Reduction products	Weight loss
	$La_2W_3O_{12}$ reduced in 100% H_2 with 10 K/min	
RT–1100 K	$La_2W_{1.25}O_{6.75}$, W	6.17% /f.u.
RT–1400 K	La_2O_3, W	9.8% /f.u.
	$LaFeW_3O_{12}$ reduced in 100% H_2 with 10 K/min	
RT–1200 K	La_2WO_6, W, Fe_2W, or Fe_7W_6	14% /f.u.
RT–1500 K	La_2O_3, W, Fe_2W, or Fe_7W_6	16% /f.u.
	$LaFeW_3O_{12}$ reduced in 5% H_2 with 5 K/min	
RT–1500 K	$La_x(WO_4)_y$, W, Fe_2W or Fe_7W_6	15.2% /f.u.
	$LaFeW_3O_{12}$ crystal reduced in 5% H_2 with 5 K/min	
RT–1500 K	$La_2W_{1.25}O_{6.75}$, W, Fe_2W, or Fe_7W_6	16.2% /f.u.

[a] RT, room temperature.

formation of W metal followed by the reduction of $FeWO_4$ to an Fe–W alloy plus W.

6. CONCLUSIONS

The described novel lanthanum tungstates, in particular the phase $LaFeW_3O_{12}$, represent the first members of a class of layered composite structural frameworks. Further members have been and will be synthesized as well as characterized based on the following approach.

Compositional Variations

The lanthanum position can be substituted by other rare earth metal cations. This leads to a fine-tuning of composition and structure. Analogous replacements of the tungsten position by molybdenum have been carried out successfully (15). The most interesting potential variation to be tried is based on the substitution of the iron position by other 3*d* and 4*d* transition metals. This does not only allow the synthesis of mixed-valence compounds leading to pronounced changes of physical properties such as conductivity or magnetism, it also leads to the possibility of modifying the chemical reactivity, in particular under reducing atmosphere. Consequently a whole range of interesting intermediate and product phases can be expected.

Structural Variations

As has been mentioned, there are indications of alternating stacking sequences of the $Fe_2W_4O_{15}$ layers and the $La_2W_2O_9$ layers along the crystallographic *c* axis. The substitution of the metal cations as well as the alteration of the compositional ratios may lead to the formation of a homologous series as observed in, e.g., the Aurivillius phases.

The results of these variations will provide further detailed insights into the interrelation between composition, structure, physicochemical properties, and reactivity of complex metal oxides.

REFERENCES

1. B. Aurivillius, *Ark. Kemi* **2,** 519 (1950).
2. G. N. Subbana, T. N. Guru Row, and C. N. R. Rao, *J. Solid State Chem.* **86,** 206 (1990).
3. S. N. Ruddlesden and P. Popper, *Acta Crystallogr.* **10,** 538 (1957); **11,** 54 (1958).
4. C. N. R. Rao, J. Gopalakrishnan, and K. Vidyasagar, *Indian J. Chem. A* **23,** 265 (1984).
5. C. N. R. Rao and J. M. Thomas, *Accounts Chem. Res.* **18,** 113 (1985).
6. F. Lichtenberg, D. Widmer, J. G. Bednorz, T. B. Williams, and A. Reller, *Z. Phys. B* **82,** 211 (1991).
7. F. Lichtenberg, D. Widmer, J. G. Bednorz, T. B. Williams, and A. Reller, *Z. Phys. B* **84,** 369 (1991).
8. T. B. Williams, F. Lichtenberg, A. Reller, and J. G. Bednorz, *J. Solid State Chem.* **103,** 375 (1993).
9. K. Nassau, H. J. Levinstein, and G. M. Loiacono, *J. Phys. Chem. Solids* **26,** 1805 (1965).
10. D. T. Templeton and A. Zalkin, *Acta Crystallogr.* **16,** 762 (1963).
11. J. Lange and H. Burzlaff, *J. Appl. Crystallogr.* **24,** 190 (1990).
12. D. Abeln and J. Kopf, 16th IUCr-Congress, Beijing, China, 1993, Collected Abstracts, PS-02.06.01, p. 43.
13. G. M. Sheldrick, *Acta. Crystallogr. Sect. A* **46,** 467 (1990).
14. G. M. Sheldrick, *J. Appl. Crystallogr.*, in preparation.
15. D. Abeln, M. Gärtner, and A. Reller, in preparation.